EJFA Emirates Journal of Food and Agriculture

Emirates Journal of Food and Agriculture 38: e213879
doi: 10.3897/ejfa.2026.213879

RESEARCH PAPER

Context-dependent cereal defense and the limits of TRI-cluster transcription as a proxy for deoxynivalenol: A cross-study transcriptomic analysis

Yao Yu[1], Yixiao Yang[1], Chunzhe Yang[1], Xiangru Wang[1], Junzhu Wang[1]

1 *New Product Development Department, China Resources Beverage (Holdings) Company Limited, Shenzhen High-tech Industrial Park (North District), 22 Langshan Road, Nanshan District, Shenzhen, Guangdong Province 518057, China*

Corresponding author: Yao Yu (yucrbeverage@163.com)

Academic editor: Mohamed Mannaa ♦ **Received** 31 August 2026 ♦ **Accepted** 15 September 2026 ♦ **Published** 12 October 2026

Abstract

Deoxynivalenol (DON) can enter cereal-derived beverages through contaminated ingredients, yet RNA measurements do not quantify toxin burden. We reanalyzed eight public barley, wheat, and *Fusarium graminearum* transcriptomic series while retaining each study's design. The analysis included 251 sample-level profiles plus public comparison-level fungal data. At 48 h in barley, eight of 344 eligible Gene Ontology pathways passed discovery-stage bidirectional rules; all eight happened to be upward. Three pathways, including glutathione and aromatic amino acid metabolism, had both purified-DON-associated and infection-associated support, whereas five represented broader infection responses. Seven non-phenylpropanoid pathways remained upward across all 77 pathway-by-contrast tests after limiting each barley gene to one wheat ortholog, although 72 retained false-discovery-rate (FDR) support. In the original exploratory gene screen, eight barley–wheat ortholog pairs were positive across studies; six remained after applying BH FDR < 0.05 to the direct-DON component, and five were also homeolog-concordant. A later barley chemotype dataset yielded no FDR-significant eligible pathway, but its cultivar, chemotype, time, mapping coverage, and sample size limit interpretation. Fungal TRI-cluster transcription increased after FgSfp1 deletion, whereas the source study separately reported 95.4% lower DON yield. This directional comparison was not a matched transcript-toxin calibration. Host pathways and fungal TRI RNA describe context-dependent biological states, not chemical DON concentration. Their possible beverage relevance is limited to upstream hypothesis generation and prioritization of chemical testing.

Keywords

Cereal-derived beverages, deoxynivalenol, *Fusarium graminearum*, glutathione, transcriptomics, TRI cluster

Introduction

Deoxynivalenol (DON) is a trichothecene mycotoxin produced predominantly by *Fusarium* species that colonize cereal crops (Pestka 2010; EFSA Panel on Contaminants in the Food Chain (CONTAM) et al. 2017). Wheat, barley, oats, and their fractions are not only staple foods and feed ingredients but also raw materials for cereal-derived beverages. Consequently, contamination originating in the crop can remain relevant after ingredient selection and processing. In a survey of 72 commercial plant-based beverages, 64% contained at least one of the targeted mycotoxins and DON was among the most frequently detected (Pavlenko et al. 2024). A controlled oat-beverage study subsequently reported 66–78% transfer of DON from flour to the liquid product, final concentrations of 89–228 μg/L

Copyright *Yu, et al.* This is an open access article distributed under the terms of the Creative Commons Attribution License (CC-BY 4.0), which permits unrestricted use, distribution, and reproduction in any medium, provided the original author and source are credited.

under the tested formulations, and no significant reduction after conventional sterilization (Teixido-Orries et al. 2025). Transfer and transformation across a barley-to-malt-to-beer chain provide a second cereal-beverage example (Lancova et al. 2008). These studies do not establish prevalence in every market or process, but they show why upstream cereal biology and downstream chemical measurement must be connected without being conflated.

That distinction is operationally important. Representative sampling and validated, matrix-specific chemical analysis are required to establish toxin concentration in an ingredient or finished product. By contrast, host and fungal RNA can report biological states associated with exposure, infection, or toxin biosynthesis. Transcriptomics may therefore help explain source biology, prioritize raw materials or conditions for targeted testing, and evaluate candidate interventions at a mechanistic level. It cannot, on its own, establish processing removal, regulatory compliance, exposure, or lot-release suitability.

In wheat and barley, *Fusarium graminearum* causes *Fusarium* head blight (FHB), reducing yield and end-use quality while increasing mycotoxin risk. Host responses include pathogen recognition, oxidative-stress control, cell-wall modification, specialized metabolism, and xenobiotic detoxification (Kazan and Gardiner 2018). Recent barley studies show that the magnitude and modular composition of host transcription depend on genotype and environment; matched transcript, protein, and metabolite measurements also implicate aromatic amino acid-derived defense metabolism during FHB (Hoheneder et al. 2023; Hein et al. 2026). Earlier barley experiments provide complementary perturbations: infection with a DON-producing wild type or a trichothecene-deficient tri5 mutant, direct application of purified DON, and an independent infection time course (Boddu et al. 2006, 2007; Gardiner et al. 2010). The wild-type-versus-tri5 contrast changes fungal DON capability, but tri5 deletion may also alter fungal physiology, biomass, and host–pathogen interactions. We therefore use it only as a DON-capability contrast. Evidence from purified DON is described as a direct-DON-associated host response, and infection contrasts are interpreted separately. The legacy microarray platform and older gene annotation also complicate comparison with current RNA-sequencing studies.

The corresponding interpretive problem on the pathogen side concerns the TRI biosynthetic cluster. Core TRI genes are mechanistically linked to trichothecene biosynthesis and are often induced under toxin-promoting or *in planta* conditions. Actual DON output also depends on translation, precursor supply, cellular state, fungal biomass, substrate, and environment. Chemotype comparisons show that transcriptional differences do not map uniformly to DON accumulation across host genotypes (Puri et al. 2016). TRI RNA may therefore describe a toxin-associated fungal state without supplying a quantitative toxin measurement.

Public repositories contain complementary cereal and fungal transcriptomic experiments spanning host species, cultivars, tissues, chemotypes, time points, and genetic perturbations (Clough et al. 2024). These data permit a stringent recurrence test if each study retains its own design and statistical model. Pooling normalized expression values across platforms, or treating dependent contrasts as independent observations, would create precision that the experiments do not support. Identifier mapping is another source of uncertainty that must remain visible.

We therefore used a cross-study framework with three components rather than a classical meta-analysis. First, barley discovery analyses identified direct-DON-associated and broader infection-associated pathways. Second, the pathways defined at the discovery stage were carried unchanged into independent wheat and barley datasets, with explicit mapping and wheat-homeolog sensitivity analyses. Third, fungal TRI-cluster transcription was examined across three sources and compared directionally with an external published DON phenotype. Across eight GEO series, the analysis comprised 251 sample-level profiles plus comparison-level fungal files. The objective was not to derive a diagnostic biomarker, infer causality, or predict DON concentration. It was to identify recurrent biological states, show where they did not transfer, and define a bounded potential application to cereal raw-material investigation.

Materials and methods

Abbreviations

3ADON, 3-acetyldeoxynivalenol chemotype; **15ADON**, 15-acetyldeoxynivalenol chemotype; **BH**, Benjamini–Hochberg; **DON**, deoxynivalenol; **FDR**, false discovery rate; **FHB**, *Fusarium* head blight; **GEO**, Gene Expression Omnibus; **GO**, Gene Ontology; **NIV**, nivalenol; **PCA**, principal component analysis; **TPM**, transcripts per million.

Study design and public data

Three Morex barley microarray series formed the discovery component. GSE33398 contained 18 inflorescence arrays (n = 3 per treatment–time cell) for water, a trichothecene-deficient *F. graminearum* tri5 mutant, and the DON-producing wild type at 48 and 96 h. GSE33405 contained 24 floret arrays (n = 3 per cell) for purified DON or water at 1, 12, 24, and 48 h. GSE33407 contained 44 inflorescence arrays (n = 4–5 per cell) for *F. graminearum* infection or water from 24 to 144 h (Boddu et al. 2006, 2007; Gardiner et al. 2010).

The context and validation studies differed substantially. GSE174081 contributed 48 processed-TPM barley grain profiles (n = 3 per cultivar–treatment–time cell) from CDC Kendall and Norman exposed to 3ADON, 15ADON, NIV, or mock conditions at 72 and 96 h (Tucker et al. 2021). GSE118126 contributed 93 mixed host/pathogen raw-count libraries from four wheat cultivars, lemma and rachis tissues, and 1–4 days after infection; primary inference used the matched infection-versus-water cells at

2 days, generally n = 3. GSE233409 contributed 18 wheat spikelet libraries (n = 3 per cultivar–condition cell) from three winter-wheat cultivars at 7 days; nine infected dual-RNA-sequencing libraries also supplied a nested fungal matrix (Wang et al. 2018; Walker et al. 2024).

Additional fungal analyses used six processed-FPKM GSE262607 mycelial profiles (three FgSfp1 knockout and three PH-1 wild type) and 10 public GSE83735 Cuffdiff comparison files representing 16 source libraries across 3ADON/15ADON, culture/*in planta*, and 48–144 h contexts (Puri et al. 2016; Sun et al. 2024). For GSE262607, RNA sequencing used 3-day liquid trichothecene-biosynthesis-inducing cultures at 25 °C with shaking, whereas the source article's liquid-chromatography–tandem-mass-spectrometry DON assay used 7-day potato-dextrose-agar cultures at 28 °C. Thus, the genotype contrast was shared, but medium, culture format, temperature, duration, and samples differed. We used the chemical result only as external source-study context; it was not remeasured, paired sample by sample, or treated as directly quantitatively comparable with the public FPKM profiles.

All files were obtained from GEO or linked public annotation repositories. The 29 downloaded files represented 267 GEO records. Sample-level analyses retained 251 profiles across seven series; the nine GSE233409 fungal profiles were nested within the 18 dual-RNA-sequencing libraries and were not counted again. GSE83735 contributed comparison-level rather than replicate-level data. Table 1, Suppl. material 1: table S8 report cultivar or strain, tissue, pathogen or chemotype, time, cell size, platform, value type, model, and the principal comparability limit. These differences can alter power, eligible genes, effect magnitude, and apparent direction, so no expression matrix, effect size, or P value was pooled across studies. Suppl. material 1: table S1 provides file identities, URLs, sizes, and SHA-256 checksums.

Metadata reconciliation and quality control

Sample labels were reconciled among GEO MINiML records, matrix column names, and the corresponding publications. Species, tissue, cultivar or strain, treatment, time, biological replicate, data level, and matrix type were recorded before modeling. Each study was processed separately; no cross-study batch correction or pooled expression matrix was used.

Quality control included expression-distribution inspection, PCA, sample–sample correlation, within-group correlation, library size, and normalization factors where applicable. A preliminary RNA-sequencing warning required both a within-group correlation deficit greater than 0.05 relative to the group median and an absolute within-group correlation below 0.80. Microarray warnings also considered array intensity and interquartile-range behavior. Warnings did not trigger automatic exclusion, and primary analyses retained all samples. Influence analyses then excluded GSM5285875 and GSM5285877 from GSE174081 and GSM3318979 and GSM3319003 from GSE118126. GSE33398 sample GSM826283 was retained because its isolated interquartile-range warning was not supported by the full quality-control profile.

Barley microarray preprocessing and differential expression

The three Barley1 series were analyzed from public processed MAS5 matrices because a complete, harmonized CEL-level reprocessing route was not available for this analysis. Values were log2 transformed, and each study was modeled independently with limma empirical-Bayes linear models (Ritchie et al. 2015). At the common 48-h window, five contrasts were evaluated: purified DON versus water in GSE33405; DON-producing wild type versus water, tri5 mutant versus water, and wild type versus tri5 mutant in GSE33398; and independent *F. graminearum* infection versus water in GSE33407. Later contrasts supplied temporal context. The wild-type-versus-tri5 result was interpreted as a DON-capability contrast rather than a DON-specific causal effect.

Barley1 probe sequences were mapped to Ensembl Plants release 63 Morex V3 complementary DNA by exact forward-strand 25-mer matching. Transcript isoforms were collapsed to genes. A unique high-confidence assignment required a probe set's constituent probes to support one gene under the documented mapping rules; moderate, ambiguous, low-support, and unmapped categories remained visible in the audit. Multiple high-confidence probe sets for one gene were collapsed by the sample-wise median. The common discovery universe contained 11,310 Morex V3 genes. For GSE174081 and GSE118126, legacy identifiers were linked to current annotations with evidence classes; unique high-confidence links defined primary results, and high-plus-moderate links defined mapping sensitivity analyses. Many-to-one count mappings were summed before filtering, whereas processed expression features were collapsed as documented in the reproducibility scripts. Differentially expressed genes were defined as BH FDR < 0.05; an additional summary required absolute log2 fold change ≥ 1 (Benjamini and Hochberg 1995). Mapping losses were quantified at the feature, gene-universe, and pathway-member levels (Suppl. material 1: tables S2, S11).

Pathway discovery and decomposition

GO Biological Process annotations were obtained from Ensembl Plants release 63 (Yates et al. 2026), with Morex V3 serving as the barley reference (Mascher et al. 2021). Gene sets contained 10–500 genes in the tested expression universe. Competitive pathway tests used CAMERA with an intergene correlation of 0.01 and trend variance modeling (Wu and Smyth 2012). P values were adjusted within each contrast by the BH method.

Table 1. Public transcriptomic datasets and analytical roles.

Accession	Organism	Profiles and cell size	Tissue and cultivar or strain	Exposure, chemotype, and time	Platform and value type	Primary role and comparison	Statistical method	Principal cross-study limit
GSE33398	*Hordeum vulgare*	18 Barley1 MAS5 arrays; n=3 per treatment-time cell	inflorescence; Morex	*F. graminearum* DON-producing wild type, DON-deficient tri5 mutant, and water; DON_capability_ contrast; 48 h; 96 h	GPL1340; MAS5_ signal	barley DON-capability and infection decomposition; 48-h wild-type infection versus water, tri5-mutant infection versus water, and wild type versus tri5 mutant	limma on log2 MAS5 after high-confidence Barley1-to-Morex v3 remapping; CAMERA	Wild type versus tri5 is a DON-capability contrast and can also reflect fungal physiology, biomass, or host-pathogen interaction changes.
GSE33405	*Hordeum vulgare*	24 Barley1 MAS5 arrays; n=3 per treatment-time cell	floret; Morex	purified DON application and water; DON; 1 h; 12 h; 24 h; 48 h	GPL1340; MAS5_ signal	direct-DON discovery; 48-h direct DON versus time-matched water for discovery; earlier times provide context	limma on log2 MAS5 after high-confidence Barley1-to-Morex v3 remapping; CAMERA	Purified-toxin exposure is not equivalent to infection, and MAS5 values are processed microarray intensities.
GSE33407	*Hordeum vulgare*	44 Barley1 MAS5 arrays; n=4-5 per treatment-time cell	inflorescence; Morex	*F. graminearum* infection and water; source chemotype not resolved in the matrix metadata used here; not reported; 144 h; 24 h; 48 h; 72 h; 96 h	GPL1340; MAS5_ signal	independent barley infection series; 48-h infection versus water for independent barley infection support; full time course provides context	limma on log2 MAS5 after high-confidence Barley1-to-Morex v3 remapping; CAMERA	One cultivar and a legacy processed microarray platform limit generalization.
GSE174081	*Hordeum vulgare*	48 TPM profiles; 16 cultivar-treatment-time cells with n=3	grain; CDC Kendall; Norman	3ADON-, 15ADON-, or NIV-chemotype *F. graminearum* isolates and time-matched mock; 15ADON; 3ADON; NIV; 72 h; 96 h	GPL28029; TPM	barley cultivar/ chemotype/time context validation; chemotype infection versus time-matched mock within cultivar at 72 and 96 h	limma on log2(TPM+0.5), strict mapping primary and broader mapping sensitivity; CAMERA	Processed TPM, strict mapping loss, two cultivars, later time points, isolate chemotype, and modest cell size can reduce power or alter direction.
GSE118126	*Triticum aestivum*	93 mixed host/pathogen count libraries; primary 2-d water-matched cells generally n=3	Lemma; Rachis; FL62R1; Muchmore; Stettler; Sumai3	3ADON-chemotype *F. graminearum* infection and water; 3ADON; 1 dpi; 2 dpi; 3 dpi; 4 dpi	GPL18862; raw_ count_mixed_host_ pathogen	independent wheat tissue/cultivar validation; infection versus time-matched water at 2 d within cultivar and tissue	edgeR quasi-likelihood by tissue, strict legacy-ID mapping primary and broader mapping sensitivity; CAMERA	Only 2 d has time-matched water controls; tissue, cultivar, legacy-ID mapping loss, and count filtering affect eligible genes.
GSE233409	*Triticum aestivum*	18 host count libraries; 9 infected libraries also contribute nested fungal profiles; n=3 per cultivar-condition cell	wheat spikelet; AC Emerson; AC Morley; CDC Falcon	3ADON-chemotype *F. graminearum* infection and water; fungal transcription measured within infected libraries; 3ADON; 0 dpi; 7 dpi	GPL18862; raw_count	independent wheat validation and fungal host-context support; infection versus water at 7 d within cultivar; nested fungal contrasts across infected cultivars	edgeR quasi-likelihood on current IWGSC counts for host and fungal matrices; CAMERA	A single 7-d endpoint and three cultivars differ from barley discovery; fungal values are relative transcription, not fungal biomass or toxin concentration.

Accession	Organism	Profiles and cell size	Tissue and cultivar or strain	Exposure, chemotype, and time	Platform and value type	Primary role and comparison	Statistical method	Principal cross-study limit
GSE262607	*Fusarium graminearum* PH-1	6 FPKM profiles; wild type n=3 and FgSfp1 knockout n=3	mycelia (hyphae); FgSfp1 knockout; PH-1 wild type	FgSfp1 knockout and PH-1 wild type in mycelial culture; not reported; RNA-seq: 3 d in liquid TBI medium at 25 °C with shaking; source-study DON assay: 7 d on PDA at 28 °C	GPL33342; FPKM	fungal regulatory-perturbation proxy stress test; FgSfp1 knockout versus wild type	limma on log2(FPKM+0.5); CAMERA and sample-score sensitivity	The RNA and DON assays used the same genotype contrast but different media, culture formats, temperatures, and durations; the small processed-expression dataset is not a sample-matched or directly comparable transcript-toxin calibration.
GSE83735	*Fusarium graminearum*	16 source libraries represented by 10 public Cuffdiff comparison files; replicate-level uncertainty unavailable to the reanalysis	Inoculated Spikelet; Mycelia; 15ADON isolate population; 3ADON isolate population	3ADON versus 15ADON isolate populations and *in-planta* versus *in-vitro* contexts; 15ADON; 3ADON; 144 h; 48 h; 96 h	GPL17573; comparison_level_ FPKM	descriptive fungal chemotype and environment context; public comparison-level 3ADON versus 15ADON and *in-planta* versus culture ratios	descriptive standardized log2 ratios from public Cuffdiff outputs; no new inferential P values	Comparison-level files do not support replicate-level uncertainty or direct pooling with sample-level models.

Note. Each public study was analyzed within its own design. No expression matrix, effect size, or P value was pooled across studies. Suppl. material 1: table S8 provides the full biological and technical summary.

The pathway decomposition used the 48-h window and the 344 GO Biological Process terms eligible in all five discovery contrasts. Both CAMERA directions were eligible. A term was direct-DON-pair supported when purified DON versus water and wild type versus tri5 each had FDR < 0.05 with the same direction. It was infection-pair supported when tri5 versus water and independent infection versus water each had FDR < 0.05 with the same direction. Composite pathways passed both pairs; infection-core pathways passed the infection pair but not the direct-DON pair. Wild type versus water was retained as corroborating total-infection evidence but was not a selection gate. Three composite and five infection-core terms qualified, and all eight happened to be upward; no downward term met the same rules (Suppl. material 1: table S9). The discovery decomposition file preceded the validation outputs, and these eight pathways were carried unchanged into validation. Because this chronology is not prospective preregistration, we use the neutral term discovery-stage-defined. These evidence classes do not imply that the wild-type-versus-tri5 contrast isolates a pure DON effect.

Barley and wheat validation

The GSE174081 TPM matrix was transformed as log2(TPM + 0.5) and analyzed with limma using cultivar-by-treatment-by-time groups. Old barley identifiers were remapped to Morex V3. Unique high-confidence assignments were primary; high-plus-moderate assignments provided a mapping sensitivity analysis. A transferred pathway required at least five mapped genes. Within each cultivar and time, 3ADON, 15ADON, and NIV conditions were contrasted separately with mock treatment. Because TPM values are processed, their mean–variance structure and inferential support are more limited than a raw-count analysis.

GSE118126 contained a mixed host/pathogen raw-count matrix. Only wheat features were retained, and old IWGSC identifiers were mapped to the current annotation. Counts from old identifiers mapping to the same current gene were summed. High-confidence assignments were primary, and high-plus-moderate assignments were a mapping sensitivity analysis. Lemma and rachis were filtered, TMM normalized, and modeled separately with robust edgeR quasi-likelihood models (Chen et al. 2025). Primary infection-versus-water inference was restricted to 2 days after inoculation, the only time with matched water controls, and was performed within each cultivar and tissue, yielding eight pathway contrasts.

GSE233409 host counts were restricted to current TraesCS features, filtered, TMM normalized, and analyzed with a robust edgeR quasi-likelihood model containing six cultivar-by-condition groups. Infection-versus-water contrasts were estimated within CDC Falcon, AC Morley, and AC Emerson. Cultivar-average and cultivar-interaction contrasts were supporting analyses. The International Wheat Genome Sequencing Consortium reference supplied the coordinate framework (IWGSC 2018).

For both wheat studies, barley pathway genes were transferred through all available Ensembl Plants confidence-1 barley-to-wheat orthologs. This primary representation preserves hexaploid homeologs but may weight a barley family more than once. We therefore reran pathway tests after retaining one available confidence-1 wheat ortholog per barley gene. Selection used the highest minimum reciprocal sequence identity, then highest mean reciprocal identity, then lexical wheat identifier; expression direction, effect, and significance were not used. CAMERA used voom-transformed expression, the filtered study-specific background, an intergene correlation of 0.01, and at least five target genes. The complete all-homeolog and one-per-family results are in Suppl. material 1: table S14.

Cross-study candidate prioritization and heterogeneity

Expression estimates and pathway tests remained dataset specific; P values were not pooled. For each discovery-stage-defined pathway, we report direction, CAMERA P value, BH FDR, target-set size, and a signed normal-score display. Cultivar-interaction contrasts describe biological heterogeneity but are not meta-analytic heterogeneity statistics.

The original exploratory ortholog-pair screen required a positive purified-DON effect at nominal P < 0.05; a positive barley total-infection effect at FDR < 0.05; positive cultivar-average effects in both GSE118126 tissues with at least one tissue at FDR < 0.05; a positive GSE233409 cultivar-average effect at FDR < 0.05; membership in a discovery-stage-defined pathway; and confidence-1 Ensembl orthology. We retained this original eight-pair set for transparency and added four sensitivity scenarios. The main FDR sensitivity replaced the nominal direct-DON gate with BH FDR < 0.05. A homeolog-family audit then examined every confidence-1 wheat ortholog of the six barley source genes across both wheat studies; missing mappings were recorded as missing, not negative. The most stringent relevant scenario also required no direction-discordant jointly measured ortholog. We label pairs as Tier 1 when direct-DON FDR stability and homeolog concordance were both present, Tier 2 when the FDR gate passed but a jointly measured homeolog was direction-discordant, and Tier 3 when direct-DON support was nominal only. These are transcriptomic candidates for experimental testing, not biomarkers, causal genes, or DON measurements (Table 2, Suppl. material 1: tables S6, S12, S13).

Fungal TRI-cluster analysis

A 12-gene core TRI set was defined from NCBI PH-1 and Ensembl Fungi/FungiDB identifiers before the fungal comparisons. GSE262607 FPKM values were transformed as log2(FPKM + 0.5) and analyzed with limma for three knockout and three wild-type profiles.

Table 2. Original cross-species transcriptomic ortholog pairs with FDR and homeolog robustness tiers.

Pair	Barley gene	Wheat gene	Functional program	Orthology and identity	Barley purified DON: log2FC (P; BH FDR)	Barley total infection: log2FC (FDR)	Wheat log2FC: lemma; rachis; GSE233409	Robustness tier	Homeolog-family interpretation
C1	HORVU.MOREX.r3.1HG0051750	TraesCS1A02G186800	Glutathione metabolism	ortholog-one2many; 87.2%	1.16 (1.50e-4; 0.0128)	1.84 (0.0025)	3.93; 6.33; 4.56	Tier 1	homeolog-concordant among jointly measured confidence-1 orthologs
C2	HORVU.MOREX.r3.1HG0051750	TraesCS1D02G189700	Glutathione metabolism	ortholog-one2one; 90.2%	1.16 (1.50e-4; 0.0128)	1.84 (0.0025)	5.59; 9.23; 6.29	Tier 1	homeolog-concordant among jointly measured confidence-1 orthologs
C3	HORVU.MOREX.r3.1HG0051800	TraesCS1B02G194600	Glutathione metabolism	ortholog-one2one; 44.5%	1.23 (3.72e-4; 0.0266)	3.46 (0.013)	6.63; 13.42; 12.99	Tier 1	homeolog-concordant among jointly measured confidence-1 orthologs
C4	HORVU.MOREX.r3.1HG0063630	TraesCS1A02G250000	Cell-wall/antifungal defense	ortholog-one2one; 92.4%	1.37 (5.36e-4; 0.0351)	2.01 (0.034)	4.11; 5.38; 6.97	Tier 1	homeolog-concordant among jointly measured confidence-1 orthologs
C5	HORVU.MOREX.r3.7HG0722940	TraesCS7A02G392800	Tryptophan/aromatic amino acid metabolism	ortholog-one2one; 96.3%	0.45 (2.43e-4; 0.019)	0.84 (0.0478)	2.34; 4.61; 4.99	Tier 1	homeolog-concordant among jointly measured confidence-1 orthologs
C6	HORVU.MOREX.r3.4HG0333410	TraesCS4A02G296300	Cell-wall/antifungal defense	ortholog-one2one; 83.5%	3.10 (3.31e-7; 7.33e-5)	2.24 (0.0191)	2.28; 3.83; 6.83	Tier 2	homeolog-sensitive: at least one jointly measured confidence-1 ortholog is direction-discordant
C7	HORVU.MOREX.r3.7HG0744250	TraesCS7A02G512300	Tryptophan/aromatic amino acid metabolism	ortholog-one2one; 84.5%	0.60 (0.0139; 0.2734)	1.43 (0.0357)	3.08; 5.45; 3.61	Tier 3	homeolog-concordant among jointly measured confidence-1 orthologs
C8	HORVU.MOREX.r3.7HG0744250	TraesCS7B02G423900	Tryptophan/aromatic amino acid metabolism	ortholog-one2one; 93.6%	0.60 (0.0139; 0.2734)	1.43 (0.0357)	3.05; 5.14; 3.89	Tier 3	homeolog-concordant among jointly measured confidence-1 orthologs

Note. BH, Benjamini-Hochberg; FDR, false discovery rate. The eight pairs retain the original exploratory screen; tiers report direct-DON FDR stability and homeolog-family sensitivity. They are not validated biomarkers or DON measurements. Suppl. material 1: tables S12, S13 provide unrounded results and all 18 confidence-1 orthologs.

We tested individual genes, a mean TRI-transcription score, and the core set by CAMERA. FPKM is processed expression, the sample size is small, and the associated source-study chemical result is not a sample-matched calibration in this reanalysis. This dataset therefore provides a directional comparison relevant to the proxy assumption, not a direct quantitative test of transcript abundance against DON yield.

For GSE83735, log2 ratios were computed from the public Cuffdiff contrast values with a 0.5 offset. Because only comparison-level files were available, direction and magnitude were described without newly calculated sample-level P values. GSE233409 fungal counts from the nine infected libraries were filtered, TMM normalized, and modeled with robust edgeR quasi-likelihood methods across the three host-cultivar environments. These contrasts describe the relative fungal transcriptome. They do not estimate absolute fungal biomass or DON concentration.

External beverage-context evidence

To delimit a possible downstream application, we used three primary studies as descriptive examples of commercial occurrence, controlled oat-beverage manufacture, and barley-to-malt-to-beer transfer (Lancova et al. 2008; Pavlenko et al. 2024; Teixido-Orries et al. 2025). Their reported values were transcribed to the Fig. 7 source data. They were not pooled, treated as a systematic review, or analyzed inferentially, and no beverage sample or process was studied here.

Reproducibility and statistical reporting

Analyses were performed in R 4.5.3 with limma 3.64.3 and edgeR 4.6.3. For every principal pathway contrast, we report CAMERA target-set size, direction, P value, and BH FDR. We also summarize the modeled gene-level log2 fold changes of the exact CAMERA members by mean, median, interquartile range, range, positive fraction, and gene-level FDR fraction. These descriptive distributions are not CAMERA effect estimates and should not be compared in absolute scale across platforms. Reconstructed membership matched CAMERA target-set size in all 240 reported rows. The supplementary workbook includes the source manifest, mapping audit, 344-term bidirectional selection audit, all principal pathway statistics, mapping-coverage sensitivity, candidate robustness and homeolog-family audits, and homeolog-balanced pathway results (Suppl. material 1: tables S1–S14). Scripts, inputs or regeneration pointers, hashes, contrast definitions, and R session information are included in the reproducibility package. Unless stated otherwise, significance was FDR < 0.05. No simulated data, imputed phenotype, or inferred chemical toxin value entered the conclusions.

Results

The analysis separated discovery, replication, and assessment of the TRI proxy

The analysis incorporated eight public series, three host expression formats, and three fungal evidence types (Table 1, Fig. 1, Suppl. material 1: table S8). The 251 sample-level profiles comprised 18 GSE33398 arrays, 24 GSE33405 arrays, 44 GSE33407 arrays, 48 GSE174081 profiles, 93 GSE118126 libraries, 18 GSE233409 dual-RNA-sequencing libraries, and six GSE262607 profiles. GSE83735 added 10 comparison files derived from 16 source libraries. All 29 downloaded files passed checksum verification. Biological replication was generally three per cell, except GSE33407 (four to five), while GSE83735 lacked replicate-level values. Tissues ranged from barley floret, inflorescence, and grain to wheat lemma, rachis, and spikelet; exposure contexts ranged from purified DON and DON-capable/DON-deficient infection to three chemotypes and fungal genotypes. These design differences motivated study-specific models and limit direct comparison of effect magnitudes.

Legacy identifier recovery differed markedly among platforms (Fig. 2, Suppl. material 1: tables S2, S11). Of 22,840 Barley1 probe sets, 13,411 were uniquely assigned with high confidence to Morex V3 genes; 1,032 were moderate-confidence, 276 ambiguous, 1,206 low-confidence, and 6,915 unmapped. In GSE174081, 4,390 of 12,857 legacy barley features mapped with high confidence and 2,918 with moderate confidence. In GSE118126, 10,860 of 99,386 legacy wheat features mapped with high confidence and 64,079 with moderate confidence. Strict mappings therefore defined primary inference; broader mappings quantified sensitivity rather than replacing an inconvenient primary result. The pathway-level impact varied: broader mapping preserved direction in most contrasts but reversed the GSE118126 phenylpropanoid pattern.

The quality-control review did not justify automatic exclusion. The barley arrays showed one interquartile-range warning, GSE174081 contained two correlation warnings, and GSE118126 contained two warnings under strict mapping. No sample was flagged in GSE233409 or GSE262607. Excluding the four RNA-sequencing warnings preserved all 12 dataset-by-pathway support classifications evaluated (Suppl. material 1: table S7).

Direct DON exposure marked a nested component of the barley infection response

At 48 h, the high-confidence barley universe contained 11,310 genes. Total infection by the DON-producing strain produced 107 genes at FDR < 0.05 and 104 after also applying an absolute log2 fold-change threshold of 1; 102 of those 104 genes were upregulated (Fig. 3A). Infection by the DON-deficient tri5 mutant produced 13 genes under both criteria, all upregulated. No individual gene met FDR < 0.05 in the wild-type-versus-mutant comparison. Direct

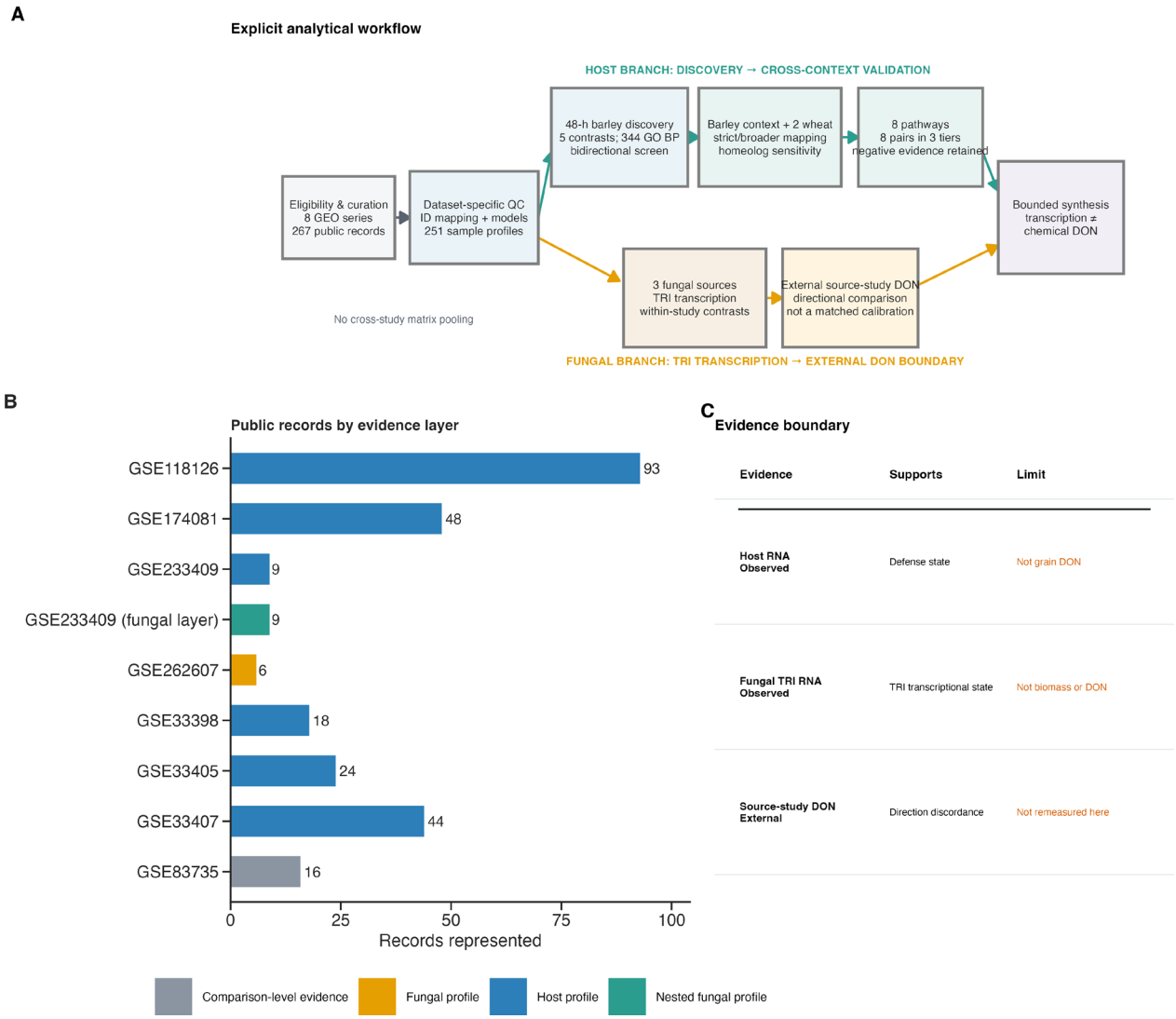

Figure 1. Public datasets and revised analytical workflow. **A.** Eligibility and curation led to dataset-specific quality control, identifier mapping, and modeling. The host branch proceeded from a bidirectional 344-term barley discovery screen to unchanged pathway transfer, mapping/homeolog sensitivity, and tiered synthesis. The fungal branch assessed TRI-cluster transcription and then placed it beside external source-study DON evidence under an explicit measurement boundary; **B.** Public records represented by host, fungal, nested-fungal, or comparison-level evidence. Eight GEO series contributed 267 records; 251 sample-level profiles entered analysis; **C.** Host RNA, fungal TRI RNA, and external chemical evidence support different claims. Matrices and P values were not pooled, and RNA was not treated as grain DON or fungal biomass.

DON application produced 206 FDR-significant genes and 142 effect-size-qualified genes, of which 132 were upregulated. The independent infection time course produced 129 FDR-significant genes and 126 effect-size-qualified genes, all upregulated. Responses were strongly time dependent: direct DON produced 4,492 FDR-significant genes at 12 h but 206 at 48 h, whereas independent infection produced none at 24 h, 129 at 48 h, and 645 at 72 h.

CAMERA detected coordinated pathway shifts despite no gene-level FDR discovery in the 48-h wild-type-versus-tri5 contrast. Of 344 jointly eligible GO terms, three met the direct-DON-pair and infection-pair rules: L-tryptophan biosynthesis, aromatic amino acid family biosynthesis, and glutathione metabolism (Fig. 3B, Suppl. material 1: tables S3, S9, S10). All were upward in the five displayed contrasts. For L-tryptophan biosynthesis (14 genes), purified DON gave CAMERA $P = 2.62 \times 10^{-4}$ and FDR = 0.018; the exact members had mean and median log2 fold changes of 0.258 and 0.239, with 64.3% positive. Wild type versus tri5 gave $P = 2.91 \times 10^{-12}$ and FDR = 1.00×10^{-9}; mean and median effects were 0.695 and 0.743, with 85.7% positive. Glutathione metabolism (47 genes) under purified DON had P = 0.00101, FDR = 0.0496, mean log2 fold change = 0.339, median = 0.090, and 59.6% positive. Complete P values, FDR values, target-set sizes, and descriptive member-effect distributions for all 240 principal rows are reported in Suppl. material 1: table S10.

Five pathways met the infection-pair rule without the direct-DON-pair rule: chitin catabolism, cell-wall macromolecule catabolism, L-tryptophan metabolism,

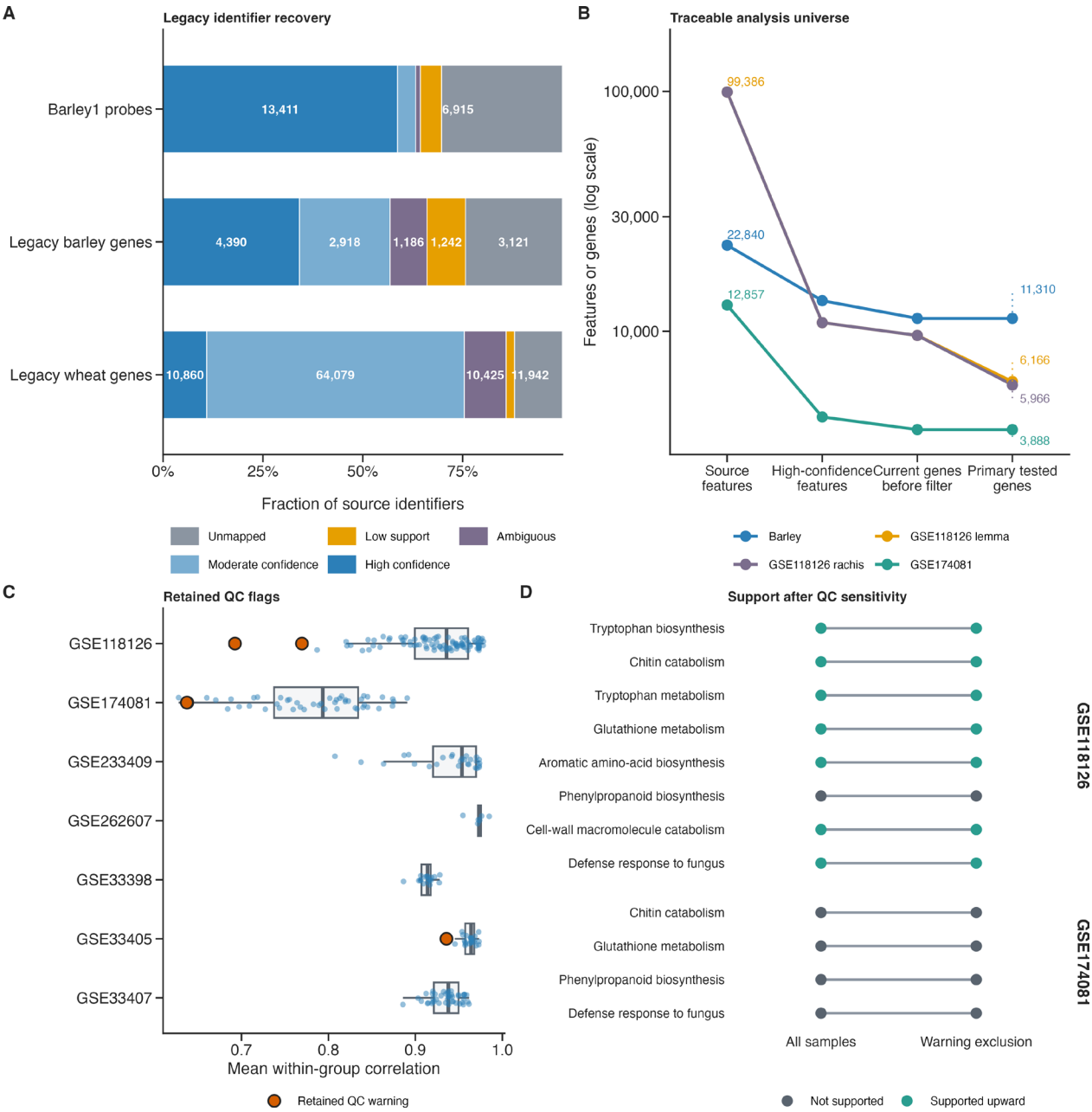

Figure 2. Identifier-mapping and sample-quality audit. **A.** Fractions and counts of Barley1 probe sets, legacy barley genes, and legacy wheat genes assigned to high-confidence, moderate-confidence, ambiguous, low-support, or unmapped categories; **B.** Attrition from source features through high-confidence mappings and current genes to the primary tested universes; the y-axis is logarithmic; **C.** Distributions of within-group sample correlations. Orange outlined points mark retained quality-control warnings; **D.** Pathway support classifications before and after warning-sample exclusion in GSE118126 and GSE174081. Teal denotes upward support and gray denotes no support under the stated rule.

phenylpropanoid biosynthesis, and defense response to fungus. Both Up and Down directions were tested; all eight qualifying pathways happened to be Up, and no Down pathway met the same criteria. Seven of eight also had total-infection FDR < 0.05. Defense response to fungus had total-infection FDR = 0.0505, illustrating that total infection was supporting evidence rather than a selection gate. The result is a direct-DON-associated metabolic component nested within a broader infection response, not a set of DON-specific pathways.

Seven discovery-stage-defined pathways transferred across two independent wheat studies

The eight discovery-stage-defined barley pathways were tested without reselection in GSE118126. With strict mapping and all available confidence-1 orthologs, seven were upward and significant at FDR < 0.05 in each of eight cultivar-by-tissue contrasts (Fig. 4A). These included the three composite and four infection-core pathways. Minimum FDR values ranged from 5.38×10^{-14} for glutathione

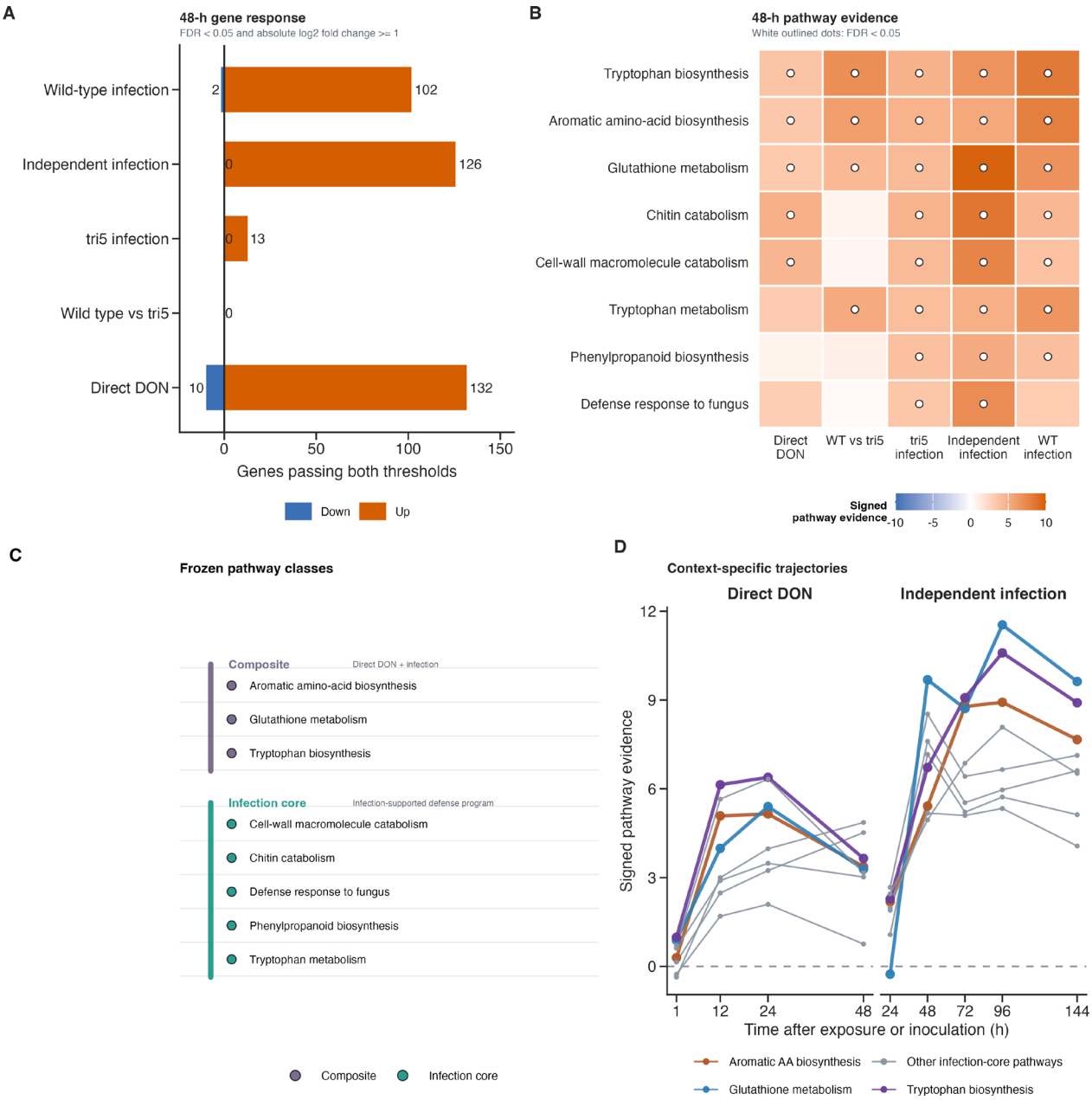

Figure 3. Barley decomposition of purified-DON-associated and infection-associated responses at 48 h. **A.** Gene counts and directions at FDR < 0.05 and absolute log2 fold change ≥ 1 in five discovery contrasts; **B.** Signed CAMERA results for the eight discovery-stage-defined GO Biological Process programs. Cell color is direction × –log10 *P*; white dots indicate FDR < 0.05; **C.** Three composite and five infection-core evidence classes. The 344-term screen admitted Up and Down directions; all eight qualifying terms happened to be Up. Total wild-type infection was supporting evidence, not a gate; **D.** Time-resolved results under purified DON and independent infection. The wild-type-versus-tri5 comparison is a DON-capability contrast that may also reflect fungal physiology or biomass; it produced no gene-level FDR discovery but did produce pathway-level shifts.

metabolism to 0.00166 for several defense-related sets. Concordance across two tissues and four resistance backgrounds supports transfer of direction beyond Morex barley, but it does not imply equal effect magnitude or independence among wheat homeologs.

Phenylpropanoid biosynthesis was the exception (Fig. 4B). Under strict mapping, it was directed downward in all eight GSE118126 contrasts, had no FDR-significant upward contrast, and had a median signed score of -0.464. When moderate-confidence legacy mappings were admitted, the pathway was directed upward in all eight contrasts and significant in seven. The apparent disagreement was therefore inseparable from the identifier-mapping rule and was classified as mapping-sensitive rather than definitively conserved or discordant.

GSE233409 supplied a second wheat validation at 7 days after inoculation (Fig. 4C). The host analysis retained 66,388 filtered genes. Infection effects differed by cultivar:

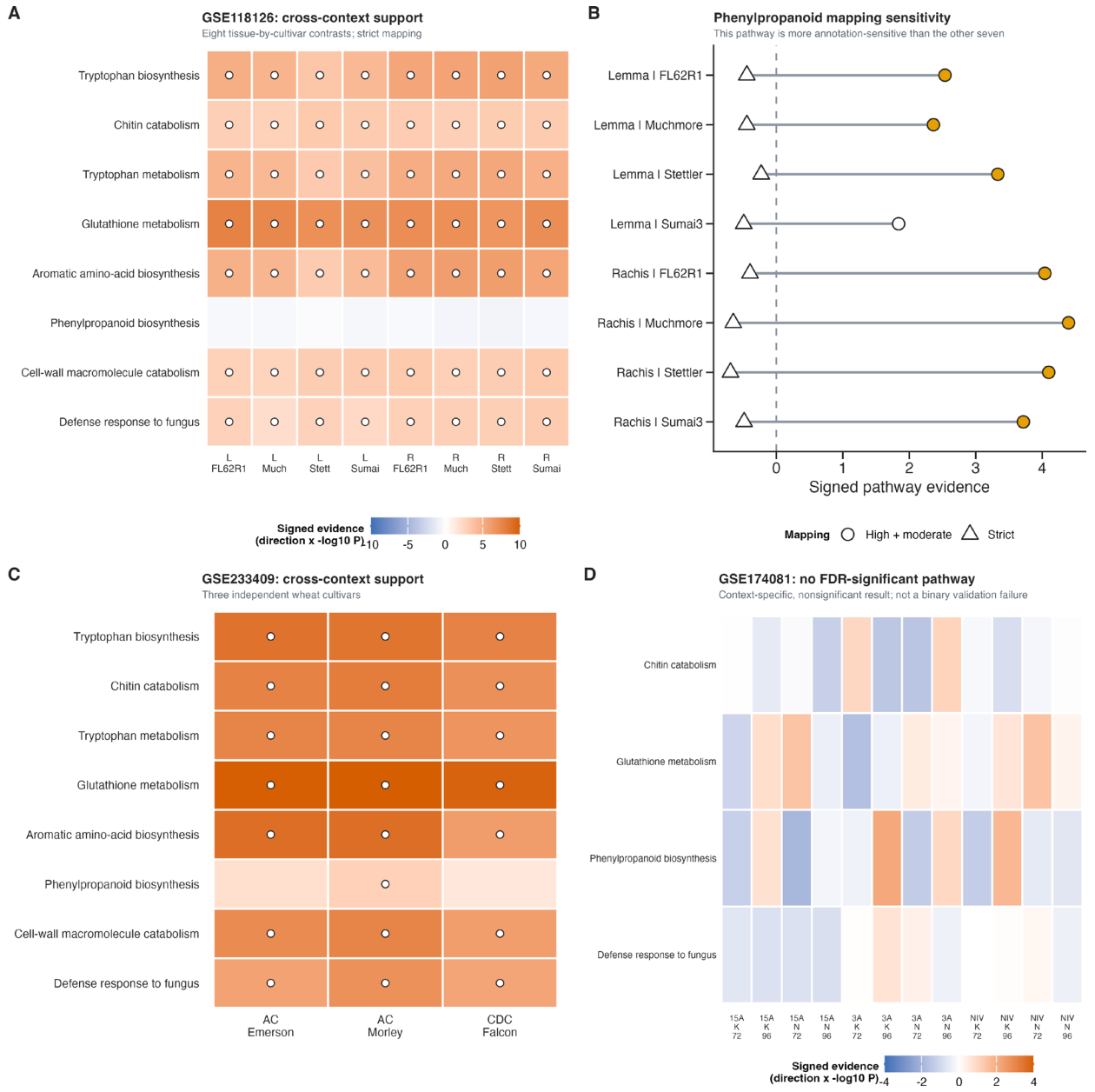

Figure 4. Independent validation and context dependence of discovery-stage-defined cereal pathways. **A.** Signed results across eight GSE118126 tissue-by-cultivar contrasts under strict mapping; **B.** Strict-mapping (triangles) and high-plus-moderate-mapping (circles) phenylpropanoid results; filled circles indicate FDR < 0.05; **C.** Three within-cultivar GSE233409 contrasts. White dots in **A** and **C** indicate FDR < 0.05; **D.** All eligible GSE174081 chemotype-by-cultivar-by-time contrasts; none met FDR < 0.05. Cell color is direction × –log10 *P*. Nonsignificant and negative results are retained; GSE174081 is interpreted as context-specific non-replication rather than biological absence.

CDC Falcon had 38,273 FDR-significant genes and 33,539 also meeting the effect-size threshold; AC Morley had 20,608 and 17,237; and AC Emerson had 28,808 and 24,053. Seven pathways were upward and significant in all three cultivars. Phenylpropanoid biosynthesis was upward in all three but significant in one. Cultivar-interaction tests identified eight significant pathway interactions in GSE118126 and six in GSE233409, so shared direction did not imply equal magnitude (Suppl. material 1: table S5).

The one-ortholog-per-barley-family sensitivity reproduced the saved all-homeolog CAMERA results for all 88 primary wheat pathway rows before changing membership (Suppl. material 1: table S14). For the seven non-phenylpropanoid pathways, direction remained Up in all 56 GSE118126 and all 21 GSE233409 contrasts. FDR < 0.05 remained in 51 of 56 and 21 of 21, respectively. Across all eight pathways, direction was preserved in 63 of 64 GSE118126 and 24 of 24 GSE233409 contrasts. The only direction change was a nonsignificant GSE118126 phenylpropanoid contrast. Thus, the main seven-pathway directional conclusion did not depend on counting multiple wheat orthologs per barley gene, although five GSE118126 significance calls weakened after balancing.

A later barley chemotype study provided no FDR-significant pathway support

Strict remapping of GSE174081 yielded 3,888 Morex V3 genes, and only four of eight pathways met the five-gene minimum. Across four eligible pathways and 12 within-cultivar, within-time contrasts per pathway, none reached FDR < 0.05 (Fig. 4D, Suppl. material 1: table S10). Directions were mixed: 19 of 48 tests were Up and 29 were Down. Glutathione metabolism was Up in seven contrasts, defense response to fungus in six, phenylpropanoid biosynthesis in four, and chitin catabolism in two; their minimum FDR values were 0.289, 0.579, 0.122, and 0.281. Broader mapping and exclusion of the two quality-control warnings did not produce general support.

This result is a context-specific non-replication under the available design, not evidence that the programs are biologically absent. GSE174081 used two different cultivars, three chemotypes, later 72–96-h sampling, processed TPM values, n = 3 per cell, and a mapping-limited universe. Any of these features can change biology, coverage, or power. We therefore retain the nonsignificant result while avoiding a universal negative conclusion.

Candidate robustness separated the original eight ortholog pairs into three tiers

The original multistudy screen yielded eight barley–wheat ortholog pairs representing six barley and eight wheat genes (Table 2, Fig. 5, Suppl. material 1: tables S6, S12). Three pairs belonged to glutathione metabolism, three to tryptophan or aromatic amino acid metabolism, and two to cell-wall or antifungal defense. Barley purified-DON log2 fold changes ranged from 0.45 to 3.10, total-infection effects from 0.84 to 3.46, and each selected wheat ortholog was positive in both GSE118126 tissues and GSE233409.

Applying BH FDR < 0.05 to the purified-DON component retained six of eight pairs and five of six barley genes. Five pairs, representing four barley genes, were also direction-concordant across every jointly measured confidence-1 wheat ortholog and were labeled Tier 1. HORVU.MOREX.r3.4HG0333410–TraesCS4A02G296300 passed the direct-DON FDR gate but was Tier 2 because another family member, TraesCS4B02G017300, was negative in GSE118126 lemma (log2 fold change = −1.38, FDR = 0.0282) and in the GSE233409 cultivar average (log2 fold change = −0.61, FDR = 1.00). The two pairs sourced from HORVU.MOREX.r3.7HG0744250 were Tier 3 because direct-DON P = 0.0139 but BH FDR = 0.273. Across the six barley families, all 18 confidence-1 wheat orthologs were audited; five families were direction-concordant among jointly measured members, while incomplete mapping was retained as missing evidence (Suppl. material 1: table S13).

For scale, the Tier-1 glutathione pair HORVU.MOREX.r3.1HG0051800–TraesCS1B02G194600 had barley log2 fold changes of 1.23 under purified DON and 3.46 under total infection, and wheat average effects of 6.63 in lemma, 13.42 in rachis, and 12.99 in GSE233409. The eight-pair set remains an exploratory record of the original screen; the tiers prevent the pairs from being presented as equally robust. None is a validated biomarker, resistance determinant, detoxification gene, or predictor of grain DON.

TRI-cluster RNA marked fungal state but not DON yield

In GSE83735, the core TRI cluster was strongly induced *in planta* relative to culture for both chemotype populations (Fig. 6A, Suppl. material 1: table S4). Median gene-level log2 ratios ranged from 4.66 to 5.89 across 48, 96, and 144 h, with 10–12 assayed TRI genes positive in each comparison. In contrast, *in-planta* 3ADON-versus-15ADON median ratios ranged from -0.629 to -0.030, and the *in-vitro* comparison was approximately zero. These comparison-level results indicated that the *in-planta* environment dominated TRI transcription, whereas chemotype differences were smaller, variable, and not accompanied by sample-level uncertainty in the public files.

The nine fungal profiles nested within GSE233409 also showed host-context dependence (Fig. 6B). Relative to the fungal transcriptome in susceptible CDC Falcon, the TRI set was increased in AC Emerson (CAMERA FDR = 1.19×10^{-6}; median core-TRI log2 fold change = 2.84) and AC Morley (FDR = 5.33×10^{-5}; median = 2.00). Emerson and Morley did not differ significantly at the set level. Because only infected libraries were available, these contrasts cannot distinguish altered fungal biomass from altered per-cell expression and cannot be interpreted as cultivar-specific DON quantities.

GSE262607 supplied a source-study directional comparison relevant to the proxy assumption (Fig. 6C, D). All 12 core TRI genes were higher in the FgSfp1 knockout, with a median gene-level log2 ratio of 3.04. CAMERA detected coordinated induction (P = FDR = 2.75×10^{-6}), and the mean TRI-transcription score increased by 3.25 log2 units (P = FDR = 0.00555). The source article separately reported 95.4% lower DON yield in the knockout (Sun et al. 2024). The public FPKM profiles and chemical result were not paired sample by sample or remeasured together here. The different assay conditions preclude attributing the apparent transcript-toxin discordance solely to genotype. This juxtaposition illustrates why transcript-only inference requires caution; it does not estimate a transcript-to-DON calibration.

Discussion

This analysis separates two questions that are often conflated: which host programs recur after purified DON and infection, and whether fungal TRI-cluster transcription can quantify toxin output. Glutathione- and tryptophan-related programs recurred within a broader infection response in two wheat studies. Homeolog-balanced analysis

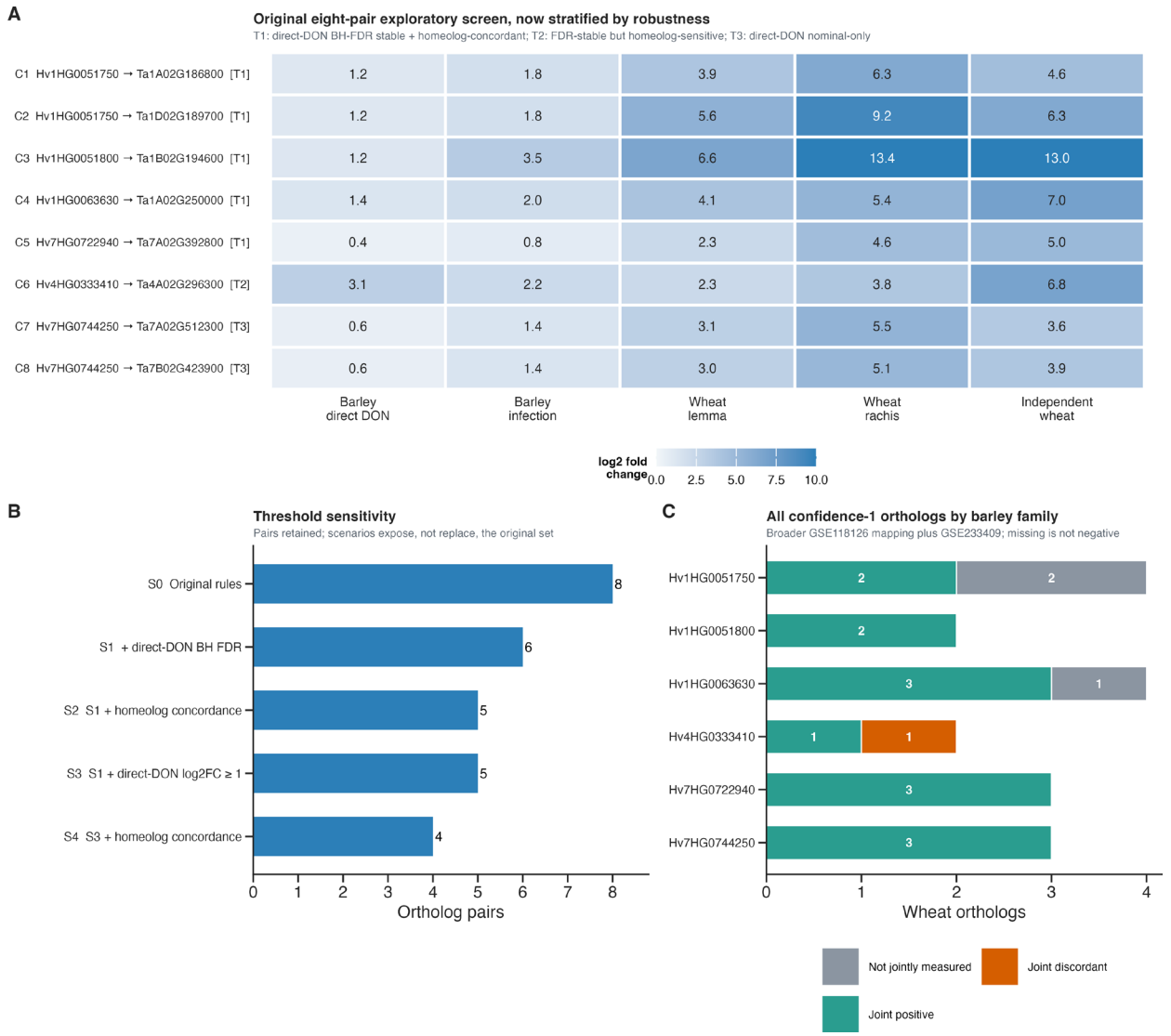

Figure 5. Robustness of the original cross-species transcriptomic candidate set. **A.** Log2 fold changes for the original eight barley–wheat pairs (C1–C8) across purified DON, barley total infection, GSE118126 lemma and rachis averages, and the GSE233409 average. T1 denotes direct-DON BH-FDR stability plus homeolog-family concordance; T2 denotes FDR stability with a direction-discordant jointly measured homeolog; T3 denotes nominal-only direct-DON support; **B.** Pairs retained under the original rules and four threshold/homeolog sensitivity scenarios; **C.** All 18 confidence-1 wheat orthologs in the six barley families, classified as jointly positive, jointly direction-discordant, or not jointly measured under broader GSE118126 mapping and GSE233409. Missing orthologs are not counted as negative. The set is exploratory and not a panel of validated biomarkers or DON measurements.

supported their direction, while mapping sensitivity and nonsignificant barley chemotype results constrained generalization. A separate source-study comparison showed that TRI transcription and reported DON yield can move in opposite directions. Transcriptomics therefore informs biological state, not toxin concentration.

The discovery design combined purified toxin application, a trichothecene-deficient mutant, total wild-type infection, and an independent infection study. It cannot turn wild type versus tri5 into a pure DON contrast: altered fungal physiology, biomass, or interaction dynamics remain possible. Its value is triangulation. No gene passed FDR < 0.05 in the 48-h wild-type-versus-tri5 contrast, yet CAMERA detected coordinated pathway shifts. The three composite pathways also responded to DON-deficient and independent infection and are therefore DON-associated within infection, not DON-specific. Glutathione can support redox buffering and conjugation, while tryptophan and aromatic amino acid metabolism can supply defense-related metabolites (Gardiner et al. 2010; Hein et al. 2026). These annotations provide biological context; no metabolite concentration, reaction flux, or toxin-removal rate was measured here.

Validation narrowed the claim. Seven pathways were Up in all eight strict GSE118126 contrasts and all three GSE233409 cultivars. They remained Up in all 77 corresponding pathway-by-contrast tests after one ortholog per barley family was retained, although five GSE118126 FDR

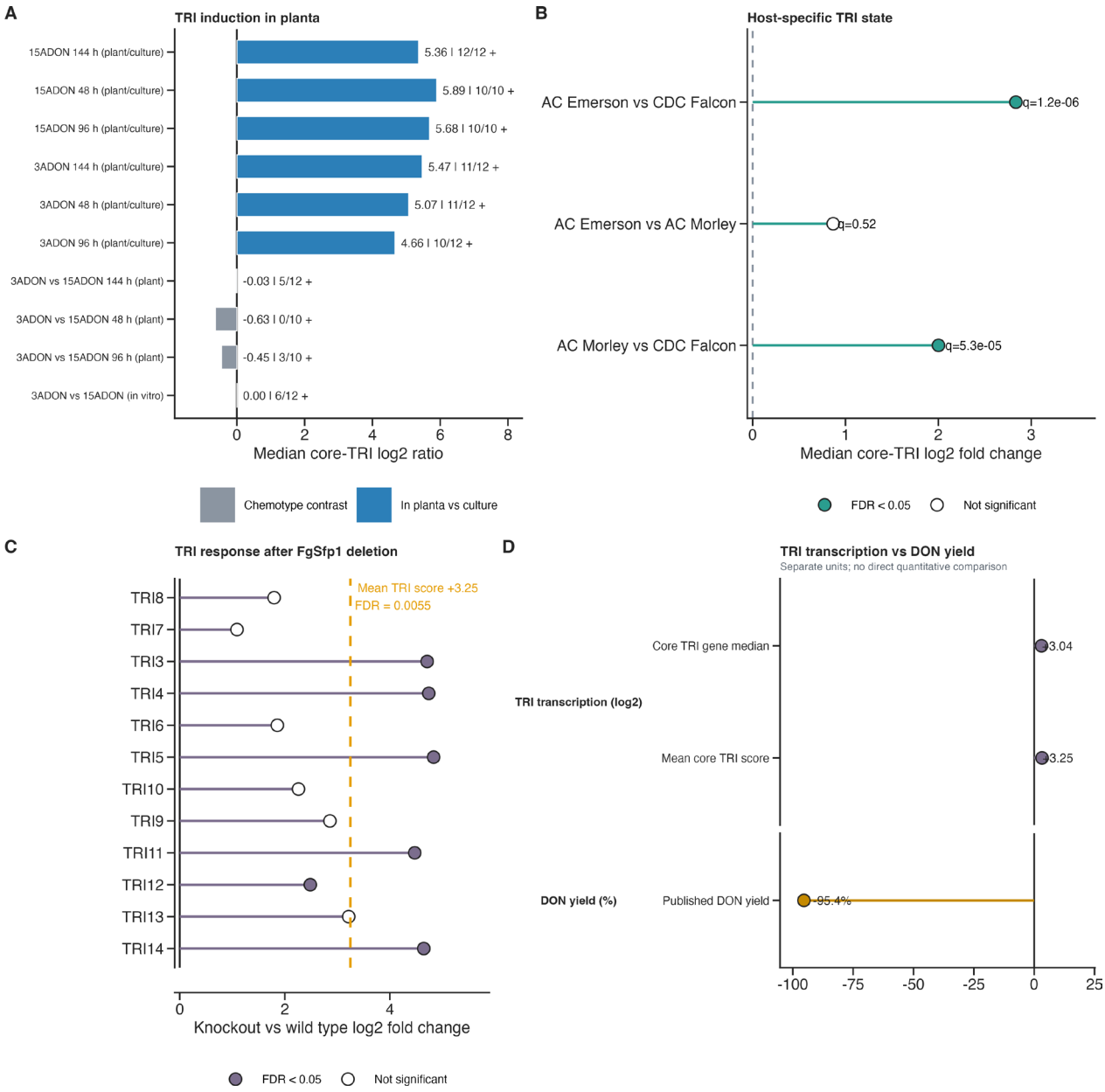

Figure 6. Fungal TRI-cluster transcription and the boundary to chemical DON. **A.** Descriptive median core-TRI log2 ratios and positive-gene counts for GSE83735 *in-planta*-versus-culture and 3ADON-versus-15ADON comparisons. Blue bars denote environmental contrasts and gray bars chemotype contrasts; **B.** Median core-TRI log2 fold changes across GSE233409 infected host cultivars; filled points indicate FDR < 0.05. These are relative fungal RNA values, not biomass or DON; **C.** TRI-gene effects after FgSfp1 deletion; filled points indicate FDR < 0.05 and the dashed line marks the mean score; **D.** Direction-only juxtaposition of higher TRI transcription and 95.4% lower DON yield reported separately by the source article. The assays used different culture conditions and sampling times. The measures are not sample-matched, share no quantitative axis, and were not generated together in this reanalysis.

calls weakened. This argues against homeolog multiplicity as the sole explanation for direction concordance. It does not eliminate incomplete mapping, unequal homeolog regulation, or cultivar heterogeneity. Significant cultivar interactions confirmed that magnitude varied among resistance backgrounds, consistent with modular barley responses (Hoheneder et al. 2023). A shared host transcriptional response is not necessarily a resistance determinant; susceptible tissue can respond strongly but late, insufficiently, or alongside greater colonization.

The retained failures are equally important. GSE174081 provided no eligible pathway at FDR < 0.05, but its later times, different cultivars and chemotypes, n = 3 profiles per cell, processed TPM values, and strict mapping loss prevent a claim of biological absence. Phenylpropanoid direction changed when moderate-confidence GSE118126 mappings were admitted and lost FDR support in the homeolog-balanced GSE233409 analysis. Its plausible role in lignification does not resolve that uncertainty. Selecting only the favorable mapping rule would be *post hoc*.

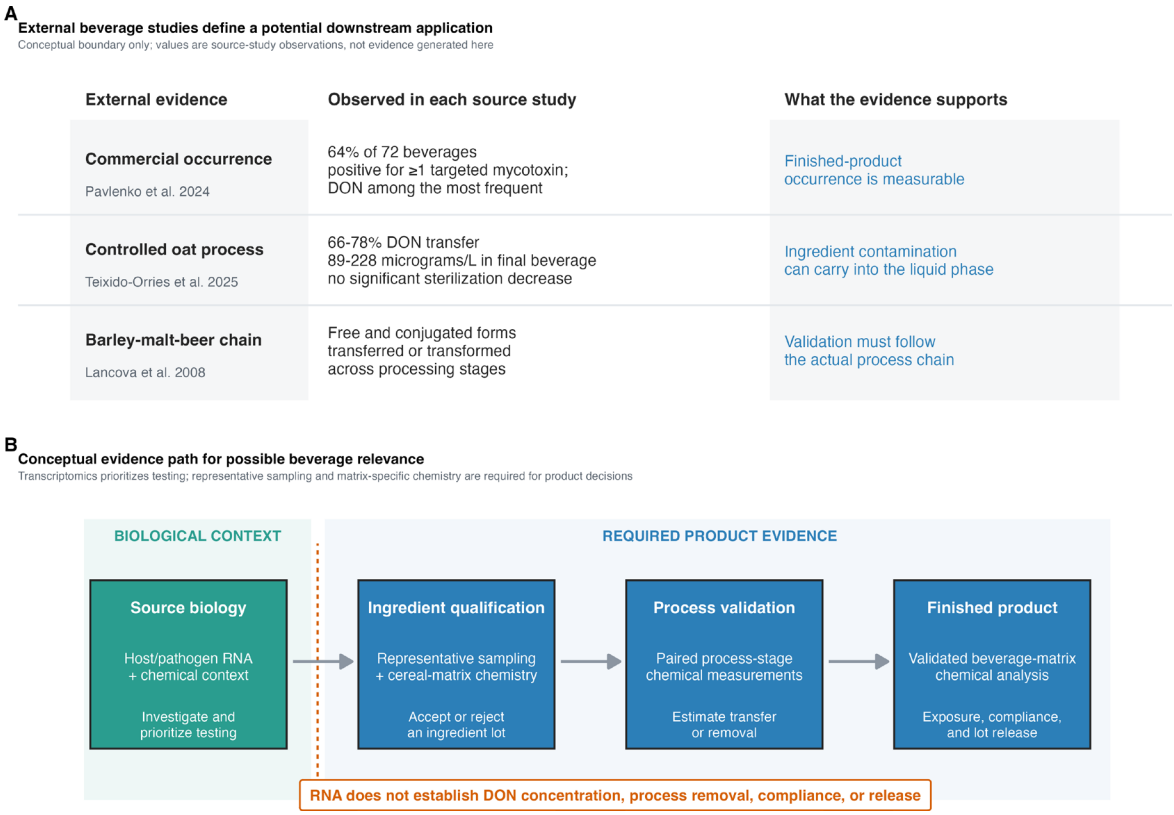

Figure 7. Conceptual evidence boundary for possible beverage relevance. **A.** Three external studies provide descriptive examples of mycotoxin occurrence or DON transfer in specific plant-based beverage, oat-processing, and barley–malt–beer contexts (Lancova et al. 2008; Pavlenko et al. 2024; Teixido-Orries et al. 2025). Values were not pooled or reanalyzed inferentially; **B.** Transcriptomics may generate upstream source hypotheses or prioritize testing, but quantitative product decisions require representative sampling and validated matrix-specific chemical analysis. The present study analyzed no beverage sample, process experiment, manufacturing lot, or new DON measurement.

Candidate sensitivity further limits interpretation. Six of eight original pairs survived direct-DON BH correction, and only five were both FDR-stable and homeolog-concordant. The tiers are more informative than an all-or-none rewrite because they preserve the original screen while exposing which evidence is fragile. Controlled inoculation, paired DON and DON-3-glucoside measurements, fungal biomass, enzyme activity, and genotype perturbation are still required. The positive-response and pathway-based screen is not an unbiased genome-wide ranking, and terms such as biomarker, resistance gene, or detoxification gene exceed the evidence.

The fungal analysis establishes the clearest measurement boundary. Strong *in-planta* TRI induction in GSE83735 marks a toxin-associated fungal environment, and GSE233409 shows host-context variation in the relative fungal transcriptome. In the separate GSE262607/source-article comparison, loss of FgSfp1 increased every core TRI transcript while reported DON yield decreased by 95.4%. The source authors proposed impaired ribosome biogenesis, lower TRI protein abundance, and altered precursor supply (Sun et al. 2024). Because the RNA and chemical assays differed in culture conditions and sampling time, this is an illustrative directional comparison rather than a matched calibration or an isolated genotype effect. It shows why coordinated biosynthetic transcripts cannot by themselves quantify DON.

The beverage implication is conceptual (Fig. 7). External studies show that DON can occur or transfer in particular beverage matrices and processes (Lancova et al. 2008; Pavlenko et al. 2024; Teixido-Orries et al. 2025). The present transcriptomic results may help formulate upstream source hypotheses or prioritize chemical testing. They do not demonstrate a beverage intervention or release tool. Ingredient qualification, process validation, exposure assessment, compliance, and lot release require representative sampling and validated matrix-specific chemical analysis.

Several limitations constrain the reanalysis. It inherited public-study sampling and preprocessing. The Barley1 series used MAS5 rather than CEL-level reprocessing; GSE174081 used processed TPM; GSE262607 used processed FPKM with three profiles per group; and GSE83735 supplied comparison files without replicate-level uncertainty. Transforming these values does not restore count-level sampling models. The 48-h discovery alignment was imperfect across tissues and exposures. GSE174081 had n = 3 per cell and a small strict-mapping universe, while GSE118126 showed substantial legacy-ID dependence. Confidence-1 orthology did not guarantee complete measurement of every wheat homeolog, and the one-per-family sensitivity addresses multiplicity but

discards real subgenome-specific information. GSE233409 fungal counts were relative and could not quantify absolute biomass. No beverage matrix, process run, commercial lot, or new chemical DON measurement was analyzed. External beverage values should not be generalized beyond their source matrices and designs.

Independent study models, strict-versus-broader mapping analyses, all-sample primary models, influence analyses, and retention of negative evidence reduce but do not remove these constraints. Dependent contrasts were not combined, and no common effect size was estimated across studies; this is not a conventional meta-analysis. The inference rests on replicated direction across distinct designs, explicit failures of transfer, and a measurement boundary that assigns transcriptomic and chemical evidence different decision roles.

Conclusions

This cross-study reanalysis identified a direct-DON-associated metabolic component within a broader infection response. Seven non-phenylpropanoid pathways retained upward direction in two wheat datasets after homeolog balancing, whereas phenylpropanoid evidence was mapping- and context-sensitive and the later barley chemotype dataset was nonsignificant. The original eight ortholog pairs separated into five FDR-stable, homeolog-concordant pairs, one homeolog-sensitive pair, and two nominal-only pairs. A source-study directional comparison also showed that higher TRI-cluster transcription can coexist with lower reported DON yield. These results generate testable host and fungal hypotheses; they do not quantify DON or establish a beverage safety outcome. Any potential beverage application requires separate representative sampling and validated chemical analysis.

Acknowledgments

The authors thank the original investigators who generated the public transcriptomic datasets analyzed in this study and the NCBI Gene Expression Omnibus for data archiving.

References

Benjamini Y, Hochberg Y (1995) Controlling the false discovery rate: A practical and powerful approach to multiple testing. Journal of the Royal Statistical Society: Series B (Methodological) 57: 289–300. https://doi.org/10.1111/j.2517-6161.1995.tb02031.x

Boddu J, Cho S, Kruger WM, Muehlbauer GJ (2006) Transcriptome analysis of the barley–*Fusarium graminearum* interaction. Molecular Plant-Microbe Interactions 19: 407–417. https://doi.org/10.1094/MPMI-19-0407

Boddu J, Cho S, Muehlbauer GJ (2007) Transcriptome analysis of trichothecene-induced gene expression in barley. Molecular Plant-Microbe Interactions 20: 1364–1375. https://doi.org/10.1094/MPMI-20-11-1364

Chen Y, Chen L, Lun ATL, Baldoni PL, Smyth GK (2025) edgeR v4: Powerful differential analysis of sequencing data with expanded functionality and improved support for small counts and larger datasets. Nucleic Acids Research 53: gkaf018. https://doi.org/10.1093/nar/gkaf018

Clough E, Barrett T, Wilhite SE, Ledoux P, Evangelista C, Kim IF, Tomashevsky M, Marshall KA, Phillippy KH, Sherman PM, Lee H, Zhang N, Serova N, Wagner L, Zalunin V, Kochergin A, Soboleva A (2024) NCBI GEO: Archive for gene expression and epigenomics data sets: 23-year update. Nucleic Acids Research 52: D138–D144. https://doi.org/10.1093/nar/gkad965

EFSA Panel on Contaminants in the Food Chain (CONTAM), Knutsen HK, Alexander J, Barregård L, Bignami M, Brüschweiler B, Ceccatelli S, Cottrill B, Dinovi M, Grasl-Kraupp B, Hogstrand C, Hoogenboom L, Nebbia CS, Oswald IP, Petersen A, Rose M, Roudot A-C, Schwerdtle T, Vleminckx C, Vollmer G, Wallace H, De Saeger S, Eriksen GS, Farmer P, Fremy J-M, Gong YY, Meyer K, Naegeli H, Parent-Massin D, Rietjens I, van Egmond H, Altieri A, Eskola M, Gergelova P, Ramos Bordajandi L, Benkova B, Dörr B, Gkrillas A, Gustavsson N, van Manen M, Edler L (2017) Risks to human and animal health related to the presence of deoxynivalenol and its acetylated and modified forms in food and feed. EFSA Journal 15: e04718. https://doi.org/10.2903/j.efsa.2017.4718

Gardiner SA, Boddu J, Berthiller F, Hametner C, Stupar RM, Adam G, Muehlbauer GJ (2010) Transcriptome analysis of the barley–deoxynivalenol interaction: Evidence for a role of glutathione in deoxynivalenol detoxification. Molecular Plant-Microbe Interactions 23: 962–976. https://doi.org/10.1094/MPMI-23-7-0962

Hein S, Steidele CE, Hoheneder F, Brajkovic S, Kuster B, Kurzweil L, Stark TD, Dawid C, Hückelhoven R (2026) Multi-omics of barley *Fusarium* head blight converge on pathogen-triggered biosynthesis of aromatic amino acid derived chemical defense compounds. Stress Biology 6: 41. https://doi.org/10.1007/s44154-026-00313-5

Hoheneder F, Steidele CE, Messerer M, Mayer KFX, Köhler N, Wurmser C, Heß M, Gigl M, Dawid C, Stam R, Hückelhoven R (2023) Barley shows reduced *Fusarium* head blight under drought and modular expression of differentially expressed genes under combined stress. Journal of Experimental Botany 74: 6820–6835. https://doi.org/10.1093/jxb/erad348

IWGSC [International Wheat Genome Sequencing Consortium] (2018) Shifting the limits in wheat research and breeding using a fully annotated reference genome. Science 361: eaar7191. https://doi.org/10.1126/science.aar7191

Kazan K, Gardiner DM (2018) Transcriptomics of cereal–*Fusarium graminearum* interactions: What we have learned so far. Molecular Plant Pathology 19: 764–778. https://doi.org/10.1111/mpp.12561

Lancova K, Hajslova J, Poustka J, Krplova A, Zachariasova M, Dostalek P, Sachambula L (2008) Transfer of *Fusarium* mycotoxins and 'masked' deoxynivalenol (deoxynivalenol-3-glucoside) from field barley through malt to beer. Food Additives & Contaminants: Part A 25: 732–744. https://doi.org/10.1080/02652030701779625

Mascher M, Wicker T, Jenkins J, Plott C, Lux T, Koh CS, Ens J, Gundlach H, Boston LB, Tulpová Z, Holden S, Hernández-Pinzón I, Scholz

U, Mayer KFX, Spannagl M, Pozniak CJ, Sharpe AG, Šimková H, Moscou MJ, Grimwood J, Schmutz J, Stein N (2021) Long-read sequence assembly: A technical evaluation in barley. The Plant Cell 33: 1888–1906. https://doi.org/10.1093/plcell/koab077

Pavlenko R, Berzina Z, Reinholds I, Bartkiene E, Bartkevics V (2024) An occurrence study of mycotoxins in plant-based beverages using liquid chromatography–mass spectrometry. Toxins 16: 53. https://doi.org/10.3390/toxins16010053

Pestka JJ (2010) Deoxynivalenol: Mechanisms of action, human exposure, and toxicological relevance. Archives of Toxicology 84: 663–679. https://doi.org/10.1007/s00204-010-0579-8

Puri KD, Yan C, Leng Y, Zhong S (2016) RNA-Seq revealed differences in transcriptomes between 3ADON and 15ADON populations of *Fusarium graminearum in vitro* and *in planta*. PLoS ONE 11: e0163803. https://doi.org/10.1371/journal.pone.0163803

Ritchie ME, Phipson B, Wu D, Hu Y, Law CW, Shi W, Smyth GK (2015) limma powers differential expression analyses for RNA-sequencing and microarray studies. Nucleic Acids Research 43: e47. https://doi.org/10.1093/nar/gkv007

Sun S, Yu D, Guo M, Tang M, Yan Z, Sun W, Wu A (2024) The transcription factor FgSfp1 orchestrates mycotoxin deoxynivalenol biosynthesis in *Fusarium graminearum*. Communications Biology 7: 1584. https://doi.org/10.1038/s42003-024-07265-4

Teixido-Orries I, Molino F, Pascari X, Ramos AJ, Marín S (2025) Impact of processing parameters and formulation on deoxynivalenol content and transfer in oat-based beverage manufacturing. LWT 218: 117368. https://doi.org/10.1016/j.lwt.2025.117368

Tucker JR, Legge WG, Maiti S, Hiebert CW, Simsek S, Yao Z, Xu W, Badea A, Fernando WGD (2021) Transcriptome alterations of an *in vitro*-selected, moderately resistant, two-row malting barley in response to 3ADON, 15ADON, and NIV chemotypes of *Fusarium graminearum*. Frontiers in Plant Science 12: 701969. https://doi.org/10.3389/fpls.2021.701969

Walker PL, Belmonte MF, McCallum BD, McCartney CA, Randhawa HS, Henriquez MA (2024) Dual RNA-sequencing of *Fusarium* head blight resistance in winter wheat. Frontiers in Plant Science 14: 1299461. https://doi.org/10.3389/fpls.2023.1299461

Wang L, Li Q, Liu Z, Surendra A, Pan Y, Li Y, Zaharia LI, Ouellet T, Fobert PR (2018) Integrated transcriptome and hormone profiling highlight the role of multiple phytohormone pathways in wheat resistance against *Fusarium* head blight. PLoS ONE 13: e0207036. https://doi.org/10.1371/journal.pone.0207036

Wu D, Smyth GK (2012) Camera: A competitive gene set test accounting for inter-gene correlation. Nucleic Acids Research 40: e133. https://doi.org/10.1093/nar/gks461

Yates AD, Austine-Orimoloye O, Azov AG, Barba M, Barnes I, Barrera-Enriquez VP, Becker A, Bennett R, Berry A, Bhai J, Bhurji SK, Branco Lins PR, Brooks L, Budhanuru Ramaraju S, Campbell LI, Carbajo Martinez M, Carpenter J, Charkhchi M, Cortes LA, Davidson C, Dickson S, Dodiya K, Donaldson S, El Houdaigui B, El Naboulsi T, Fairbrother-Browne A, Falola O, Fatima R, Gonzalez Martinez J, Gurbich T, Hall H, Hardy M, Hollis Z, Hunt T, Kay M, Kaikala V, Lazar A, Lemos D, Lodha D, Mathlouthi N, Merino GA, Merritt R, Mirabueno LP, Mushtaq A, Hossain SN, Pérez-Silva JG, Piližota I, Poppleton D, Prosovetskaia I, Raj S, Abdul Salam AI, Saraf S, Sinha S, Sipos B, Sitnik V, Suner M-M, Surapaneni L, Tierney JAS, Urbina-Gómez D, Veidenberg A, Walsh TA, Allen JM, Alvarez-Jarreta J, Cheema J, Batista da Rocha J, De Silva NH, Tricomi FF, Giorgetti S, Ilsley GR, Keatley J, Loveland JE, Mudge JM, Naamati G, Tate J, Willhoft NL, Winterbottom A, Flint BR, Frankish A, Haggerty L, Hunt SE, Clark EL, Dyer SC, Freeberg MA, Martin FJ, Finn RD (2026) Ensembl 2026. Nucleic Acids Research 54: D1053–D1060. https://doi.org/10.1093/nar/gkaf1239

Additional information

Conflict of interest

The authors have declared that no competing interests exist.

Ethical statement

This study analyzed only previously published, publicly accessible plant and fungal transcriptomic data and did not involve human participants or vertebrate animals.

Artificial Intelligence (AI) use

Regarding the use of AI in the preparation of this manuscript, the authors declare the following: GPT, OpenAI Codex.

Used for: Language, style and writing, Data analysis, Software and automation, Assessment and compliance.

During preparation of this manuscript, the authors used OpenAI Codex for public-data workflow organization, analysis-code development, quality-control checks, manuscript structuring, and language editing. All analyses, code outputs, references, interpretations, and text were reviewed and verified by the authors, who take full responsibility for the article.

Funding

No funding was reported.

Author contributions

Conceptualization: Yao Yu and Chunzhe Yang; Data curation: Yao Yu; Formal analysis: Yao Yu; Funding acquisition: Chunzhe Yang; Investigation: Yixiao Yang; Methodology: Yao Yu, Yixiao Yang, and Junzhu Wang; Project administration: Yixiao Yang; Resources: Chunzhe Yang and Junzhu Wang; Software: Yao Yu; Supervision: Yixiao Yang, Chunzhe Yang, and Xiangru Wang; Validation: Chunzhe Yang and Xiangru Wang; Visualization: Yao Yu; Writing – original draft: Yao Yu and Yixiao Yang; Writing – review and editing: Yao Yu and Yixiao Yang.

Data availability

All expression data analyzed in this study are publicly available from the NCBI Gene Expression Omnibus (https://www.ncbi.nlm.nih.gov/geo/) under accession numbers GSE33398, GSE33405, GSE33407, GSE174081, GSE118126, GSE233409, GSE262607, and GSE83735. The complete accession and file manifest, source URLs, and checksums are provided in Suppl. material 1: table S1. Analysis scripts, executed contrast definitions, mapping audits, source-data tables, software versions, and session information are included in the accompanying supplementary reproducibility package.

Supplementary material

Supplementary material 1
Supplementary tables S1–S14 (.xlsx)
Link: https://doi.org/10.3897/ejfa.2026.213879.suppl1

Supplementary material 2
Source data for Figures 1–7 (.xlsx)
Link: https://doi.org/10.3897/ejfa.2026.213879.suppl2

Supplementary material 3
Supplementary reproducibility package (.zip)
Link: https://doi.org/10.3897/ejfa.2026.213879.suppl3

Supplementary material 4
Source data for Figure 7 (CSV extract) (.csv)
Link: https://doi.org/10.3897/ejfa.2026.213879.suppl4